Occasional Note Met O 21/77/5

METEOROLOGICAL OFFICE
13 OCT 1977
LIBRARY

Velocity Measurement in a Rotating Annulus Using a Photographic Technique. Part 1. Development of a Method of Velocity Analysis

125175

by

P M Kent

Geophysical Fluid Dynamics Laboratory
Meteorological Office, Bracknell, Berkshire

August 1977

Summary

The development of an analysis technique to study velocity data derived from a pair of photographs, separated by a small intervals of time, of particles suspended in the working fluid of a rotating annulus is described. The analysis uses a Fourier series with radial polynomials to derive the velocity and energy characteristics of the flow.

Definition of Symbols

a_{jk} coefficient of the terms $x^j \sin K\Theta$ in an expansion of the velocity component.

b_{jk} coefficient of the term $x^j \cos K\Theta$ in an expansion of the velocity component.

DT time interval between each photograph

j power of radial variation of the polynomial

k wave number of the polynomial

n number of points on first photograph

r radial coordinate of each point

RIN inside radius of annulus

ROUT outside radius of annulus

x the ratio $\frac{2r - (ROUT + RIN)}{ROUT - RIN}$

u the velocity at a point

u_{jk} the velocity due to the term jk of the polynomial at a point

VMAX the maximum change in velocity considered at the start of each iteration

Θ the azimuthal coordinate of each point

1. Introduction

This report describes the development of a program for a polynomial analysis scheme to interpret pairs of photographs of illuminated neutrally buoyant particles at some level within the working fluid contained in a rotating annulus, the photographs being separated by an interval of up to one second. The positions of corresponding particles are found on each photograph and from these the velocity field is derived and analysed.

The data will be obtained from experiments on an eight centimeter radius annulus being built in the branch. It is intended that three levels or more will be investigated so that the effect of end wall topography on the flow can be studied. The aim of the laboratory investigations is to determine the factors influencing the disturbances in the flow and to determine the nature of these disturbances. The fluid velocity and energy changes obtained from the polynomial coefficients derived in the program will be used in conjunction with measurements of the temperature structure in the fluid, the physical properties of the fluid and various geometrical parameters to determine these factors.

2. The analysis scheme

a. Polynomial analysis of velocities

It is assumed that the function representing the velocity component U at a point can be expressed as the sum of a series of terms thus,

$$u = \sum_k \sum_j u_{jk} = \sum_k \sum_j (a_{jk} r^j \sin k\Theta + b_{jk} r^j \cos k\Theta) \qquad 2.1$$

where r and Θ are the radial and azimuthal coordinates of the point. j is the power of the radial variation and k the azimuthal wave number; a_{jk} and b_{jk} are the coefficients to be determined by the analysis. In practice it is convenient to replace r in equation 2.1 by x, where x=1 at the outer radius ROUT and -1 at the inner radius RIN ie.

$$x = \{ 2r - (\mathrm{ROUT} + \mathrm{RIN}) \} / (\mathrm{ROUT} - \mathrm{RIN}) \qquad 2.2$$

The analysis scheme finds the coefficients of each term in U_{jk} which minimizes the sum of the squares of the velocities, $U_n - U$, over the points, where U_n is the velocity component measured at a point $r_n\ \Theta_n$.

The equations to be solved to determine a_{jk} and b_{jk} are

$$\sum_n 2\,(u_n - u)\,\frac{\partial u}{\partial a_{jk}} = 0 \qquad 2.3$$

and

$$\sum_n 2\,(u_n - u)\,\frac{\partial u}{\partial b_{jk}} = 0 \qquad 2.4$$

On substitution of equations 2.1 and 2.2 these become

$$\sum_n \sum_j \sum_k x_n^j U_n \sin k\Theta_n = \sum_n \sum_j \sum_k \left(a_{jk} x_n^j \sin k\Theta_n + b_{jk} x_n^j \cos k\Theta_n\right) x_n^j \sin k\Theta_n \qquad 2.5$$

and

$$\sum_n \sum_j \sum_k U_n x_n^j \cos k\Theta_n = \sum_n \sum_j \sum_k \left(a_{jk} x_n^j \sin k\Theta_n + b_{jk} x_n^j \cos k\Theta_n\right) x_n^j \cos k\Theta_n \qquad 2.6$$

These apply to both zonal and radial components and are usually analysed over j=0 to 3 and k = 0 to 10.

In principle these equations could be solved simultaneously but due to the number of equations and illconditioning this was not possible. The representation of the field by an orthogonal polynomial was considered but since the particles are at random positions which vary with each pair of photographs it would have been necessary to evaluate the polynomials for each photograph although subsequent evaluation of the coefficients would have been simple. The method used was a representation as described above but in which the coefficients of the terms were evaluated individually rather than simultaneously.

The equations to be solved to determine the coefficients a_{JK} and b_{JK} are

$$\sum_n U_n x_n^J \sin K\Theta_n = \sum_n \left(a_{JK} x_n^J \sin K\Theta_n + b_{JK} x_n^J \cos K\Theta_n\right) x_n^J \sin K\Theta_n \qquad 2.7$$

and

$$\sum_n U_n x_n^J \cos K\Theta_n = \sum_n \left(a_{JK} x_n^J \sin K\Theta_n + b_{JK} x_n^J \cos K\Theta_n\right) x_n^J \cos K\Theta_n \qquad 2.8$$

The pair of coefficients of the term which then minimizes the sum of the squares

of the velocities $U_n - U_{JK}$ is found and recorded. $U_n - U_{JK}$ is then used instead of U_n and the process repeated.

If a term in the polynomial recurs during the analysis its coefficients are added to the previous values. The coefficients of the most significant term in the polynomial after each step are stored for use later with the supporting program. It was found that the analysis scheme rapidly converged to give realistic values for the coefficients.

The radial and zonal terms are treated independently and are only recombined to reconstruct the velocity fields at the end of the analysis using euation 2.1

b. Analysis of energies.

The kinetic energy density E is given by equation 2. where

$$E = \frac{1}{2}\left(U_z^2 + U_R^2\right) \qquad 2.9$$

z and R refer to the zonal and radial components. Now first just considering one component, from equation 2.1 we get

$$U^2 = \sum_k \sum_j a_{jk} x^j \sin k\theta \left(\sum_{k'} \sum_{j'} x^{j'} \left(a_{j'k'} \sin k'\theta + b_{j'k'} \cos k'\theta\right)\right) \qquad 2.10$$

$$+ \sum_k \sum_j b_{jk} x^j \cos k\theta \left(\sum_{k'} \sum_{j'} x^{j'} \left(a_{j'k'} \sin k'\theta + b_{j'k'} \cos k'\theta\right)\right)$$

By gathering terms together and using trigonometric relations equation 2.10 becomes.

$$U^2 = \sum_k \sum_{k'} \sum_j \sum_{j'} b_{jk} b_{j'k'} x^{j+j'} \cos(k+k')\theta + b_{jk} b_{j'k'} x^{j+j'} \cos(k'-k)\theta$$

$$+ b_{jk} a_{j'k'} x^{j+j'} \sin(k'+k)\theta + b_{jk} a_{j'k'} x^{j+j'} \sin(k'-k)\theta \qquad 2.11$$

$$+ b_{j'k'} a_{jk} x^{j+j'} \sin(k'+k)\theta - b_{j'k'} a_{jk} x^{j+j'} \sin(k'-k)\theta$$

$$+ a_{jk} a_{j'k'} x^{j+j'} \cos(k'-k)\theta - a_{jk} a_{j'k'} x^{j+j'} \cos(k'+k)\theta$$

which can be written

$$2u^2 = \sum_{-j} \sum_{j'} \sum_{k} \sum_{m} x^{j+j'} \Big[\big(b_{jk} (b_{j'm-k} + b_{j'm+k}) + a_{jk} (a_{j'm+k} - a_{j'm-k}) \big) \cos m\Theta + \big(b_{jk} (a_{j'm-k} + a_{j'm+k}) - a_{jk} (b_{j'm+k} - b_{j'm-k}) \big) \sin m\Theta \Big] \qquad 2.12$$

For $m+k > k_{max}$ and $m-k < 0$ coefficients are zero

Then combining the cosine coefficients and the sine coefficients of the equivalent equations for V_R^2 and V_Z^2 the amplitudes and phases of energy for each wave number m is evaluated.

3. Anslysis of the simulated velocity fields

Simulated wave number 3 flow data which qualititatively represented many of the observed features of the flow from a pair of photographs were derived using analytical expressions. These were in the form of a set of points with randomly distributed values x and Θ and the corresponding velocities. These velocities were then analysed with the polynomial scheme and the amplitudes and phases of the derived terms were compared with the expected values from the analytical data.

It was noted that for $|x| \leq 0.5$ the derived amplitudes were in good agreement with the initial data but at the edges of the annulus the amplitudes were far too large. (see figure 3.1). To overcome this edge error each radial polynomial was multiplied by the factor $(1-x^2)$ which was equivalent to assuming that the radial variation could be represented by a fifth order polynomial with the constraint that the velocity was zero at $x = \pm 1$. This brought the amplitudes to zero at the edges and left those close to the centre about the same. The analysis scheme now produced results in agreement with the initial analytical data (see figure 3.1).

Another problem was to decide on a cut-off value for the number of terms used to represent the velocity components below which only noise was being detected and for the number of iterations required to find the coefficients of these terms. Initial tests were limited to 50 iterations or to a reduction of the residual squared velocity error to one tenth of the sum of the observed square valocities. This method proved satisfactory at this stage.

4. Determination of velocities from particle positions

Having optimised the analysis program it was then necessary for an additional section to be added so that a set of velocties could be generated from the two arrays of points obtained from the photographs A and B. The difficulty is to find the point in array B which corresponded with the point in array A under consideration. This was achieved by defining a maximum velocity VMAX of the particles and looking at photograph B within a circle of radius DTx VMAX whereDT is the time interval between the photographs. If no points or more than one point existed in this circle the point from array A was ignored, and the next in the array considered. However, if only one point is found then this is noted and if when the reverse process is repeated only one point in photograph A is again found a velocity can be generated. This is defined by the separation of the points divided by DT. Hence a series of velocities can be obtained from the two photographs and these were assigned to the point mid way between the particle locations of the two photographs. The polynomial analysis was then made a subroutine of this main program and was called separately for the radial and zonal velocities.

If a large value of VMAX was chosen then only a few velocities could be determined. However, if a smaller value was chosen there were more points but the largest velocities were ignored.

In order to overcome this problem it was decided to start with a large VMAX and define an array of velocities, initially zero, which corresponded with all the array A points. The circle which was searched for points on the second photograph was assumed to be centred on points displaced by VxDT from the position in A. The small number of velocity data obtained were then analysed using the polynomial analysis scheme. The polynomials obtained were then used to derive a set of velocities for the points of array A to replace the set of zero velocities, that is,a better approximation of V is used which is not constant throughout the annulus, so that the process can be repeated. In the second and subsequent iterations the critical radius for the search circle was defined by the sum of

an error due to the rounding of the positions of the points and a value equal to twice the RMS error between the velocity fields at the start and end of the respective iteration, a measure of the accuracy of the fit of the analysed field to the original data. Thus as the error decreased with eachiteration so the circle decreased in size and its position became better known with a limit set by the rounding of the data.

Preliminary tests revealed useful information on the best method for limiting the number of terms used in the subroutine. Instead of using many terms of the polynomial to construct a velocity field given by only a few points for the first few iterations, it was noticed that, by using one term for the first [illegible] and allowing the number for subsequent ones to increase by one at a time, a much better result was achieved. This appeared to be because the polynomial could fit the small number of velocity data exactly but these velocities were not a good approximation of the true fields, only the first terms being the correct ones. Another restriction applied was to limit the number of terms to the number of points used divided by eight, thereby giving each term at least eight points to resolve it.

The main program was terminated when a specified number of iterations are completed or when both the differences between the analysed fields and the data were reduced to the rounding error of the points.

5. Test runs on program

With the program apparently working properly a series of tests were carried out each with a different wave number simulated flow or different characteristics of input data. The first set of runs were as follows:-

1. Perfect data; 200 points; K=2 flow; DT = 1.00 secs
2. Rounded data to .03 cm; 200 points; K=2 flow; DT = 1.00 s
3. No roudning; 25% random data; 200 point real data; K=2 flow, DT = 1.0 s
4. Simulation run: Rounded to .03cm; 25% random data, 200 real points; K=2 flow; DT = 1.0 s

5.6. and 7. as 4 but with gaps of $2\pi/20$, $2\pi/6$ and $2\pi/12$ in data.

The results of these runs were written to disk and the reconstructed streak photographs and amplitudes and phases of energy against x for each wavenumber plotted using programs to be described later. These were compared with each other and with the analytical results.

At first there was some difficulty in obtaining good results as it appeared that noise was being fitted particularly in radial component. Since the analytical expression for this component contained only one term noise was being fitted after the first iteration. It was therefore necessary to have separate cut-offs for the zonal and radial components and so the additional restriction that the RMS error of each component should not be less than the rounding error of the points was added. A further improvement was obtained by using an estimate of the mean zonal flow for the first iteration instead of the assumed zero flow. This then implied that the first circle was drawn a distance, defined by this velocity, from the original point. The first two iterations were also limited to wave number $K \leq 4$ but this was not made a permanent feature of the program at this stage although a similar restriction was later adopted.

The suspicion that gaps in the data would be a hindrance to the analysis was proved unfounded, runs 5, 6 and 7 producing results similar to 1,2, 3 and 4. There was very little difference between the perfect data run and the other runs, and the energy components for each wave number were in very good agreement with the analytical calculations. (see figure 6.1.). The initial set of velocities at the final step and the derived set of velocities on the grid shown in figure 6.2 for run 4.

Some problems were caused by the amount of random data which at 25% appeared to be at the limit, the analysis scheme being unable to cope with more than this. However, with 20% the scheme was very successful for the simulated K=2 flow.

The next set of tests were to study the effect of changing the number of data points. An increase in the number had little effect as did a decrease until the scheme was tested with less than 80 points. Some degradation in the results then became apparent particularly when looking at the energy plots which showed

a distinct lack of symmetry. This seemed to set a lower limit on the number required. With up to 160 points nearly all the points were used in the analysis but there was a steady percentage decrease above this probably being due to some points being too close together. Although in principle it would be better to use more data points in practice as they are not randomly distributed the optimum number appears to be between 100 and 160 as every point is then used.

The wave number K of the flow was the next parameter varied. For K=4 flow the scheme only worked for less than 15% random data, and for K=5 and 6 the flow could not be resolved at all. This appeared to be due to the increased curvature which increased the error of the velocity estimates based on a constant velocity between the two positions of the tracer particles. Thus the larger radial velocities encountered with the simulated higher wave number flows could not be resolved by the analsysis.

The final parameter to change was DT which was one second in all the above tests and can be 0.33, 0.66 or 1.00 seconds on an experimental basis. Very little difference was noted with K=2 flow but at higher wave number flow the curvature could be resolved for DT = 0.33 and 0.66 seconds since the distance traveled by the particle was much smaller (see figure 6.3). Even wave number 5 and 6 flows were resolved without prescribing the first wave chosen. On an operational basis a time interval of 0.66 second would appear to be preferable.

The final tests were to check the validity of the analysis by combining a number of flows and resolving them. The first was a straight forward combination of flows 2 and 4, and flows 2 and 5, both of which were resolved satisfactorily. The same was true when one was phase shifted relative to the other, the resolved phases of velocity and energy being as expected. The last check was to look at the system with different waves dominant in the inner and outer halves of the annulus. A weighting function, which was zero at the inner edge and one at the outer for one wave number flow and vice versa for the other, had to be applied. With a weighting function proportional to the square of the distance from one edge very goood results were obtained (see figures 6.4, 6.5, and 6.6) but one linearly

proportional to this distance some errors appeared to have crept in. However the system appears to be satisfactory and shall be left in this form for operational use.

6. Supporting programs

Two programs are used to take the analysed coefficients a_{jk} and b_{jk} off disk and convert then to useful forms. First they are recombined to produce the resolved velocity field using equation 2.1 with x instead of r. Then using Calcomp the initial field and the derived field of the final iteration are plotted, the initial field at the points used and the derived field on a circular grid of 64 points in the zonal direction and 9 in the radial.

The second program uses the coefficients to derive the amplitudes and phases of the energy in each wave no. This uses equation 2.12 for V_R^2 and V_2^2 which are combined to give the actual energy. The amplitudes and phases are plotted using Calcomp as a function of x and wave number.

7. Concluding remarks

The development of a program to analyse velocity data derived from pairs of photographs of particles suspended in a rotating fluid has been described. The analysis uses a Fourier series with radial polynomials to derive the velocity and energy characteristics of the flow.

From the photographs, separated by about a second, pairs of points are found and a set of velocities derived. These are then analysed using the above technique and the coefficients used to determine the velocities and energies due to each wave number. The determination of the points and the evaluation of the coefficients has been described. A section also describes a series of tests carried out on the program with different types of flow.

Legends to diagrams

Figure 3.1

Simulated flow of wave number 3. Analysis of zonal component of velocity. Comparison of different data; _____ analytic data, O - - O initial derived amplitudes, □ □ solution with 5th order polynomial with amplitude zero at x = ± 1.0.

Figure 6.1

Simulated flow of wave number 2. Analysis of energy components. Comparison of different data; ● — ● analitic data, × — × derived data for run 4.

Figure 6.2

Reconstruction of velocity fields at the start and end of the 4th iteration for a simulated K=2 flow. The initial field is equivalent to the array of constant velocities at the first iteration and is the same as those at the end of the 3rd. 167 points were used to derive the field (200 pts + 25% random data; rounded to .03 ; DT = 1.0 seconds)

Figure 6.3

As figure 6.2 but for K=5 flow (DT = 0.68 seconds; forced to wave number 0 or 5 for first iteration)

Figure 6.4

As figure 6.2 but for a combination flow of K=2 and K=4 with the weighting for $(r - ROUT)^2/(RIN - ROUT)^2$ applied to K=2 and $(r-RIN)^2/(R\ OUT - RIN)^2$ to K=4. (forced to wave number 0 or 2 for first step; DT = 0.68 seconds)

Figure 6.5

Amplitude and phase of energy in wave numbers 0 to 4 as a function of x for the flow in figure 6.2.

Figure 6.6

Amplitude and phase of energy in wave numbers 5 to 8 as a function of x for the flow in figure 6.2.

Figure 6.1 Analysis of energy components of simulated wave number 2 flow.
o — o analytical data, x — x derived data for run 4.

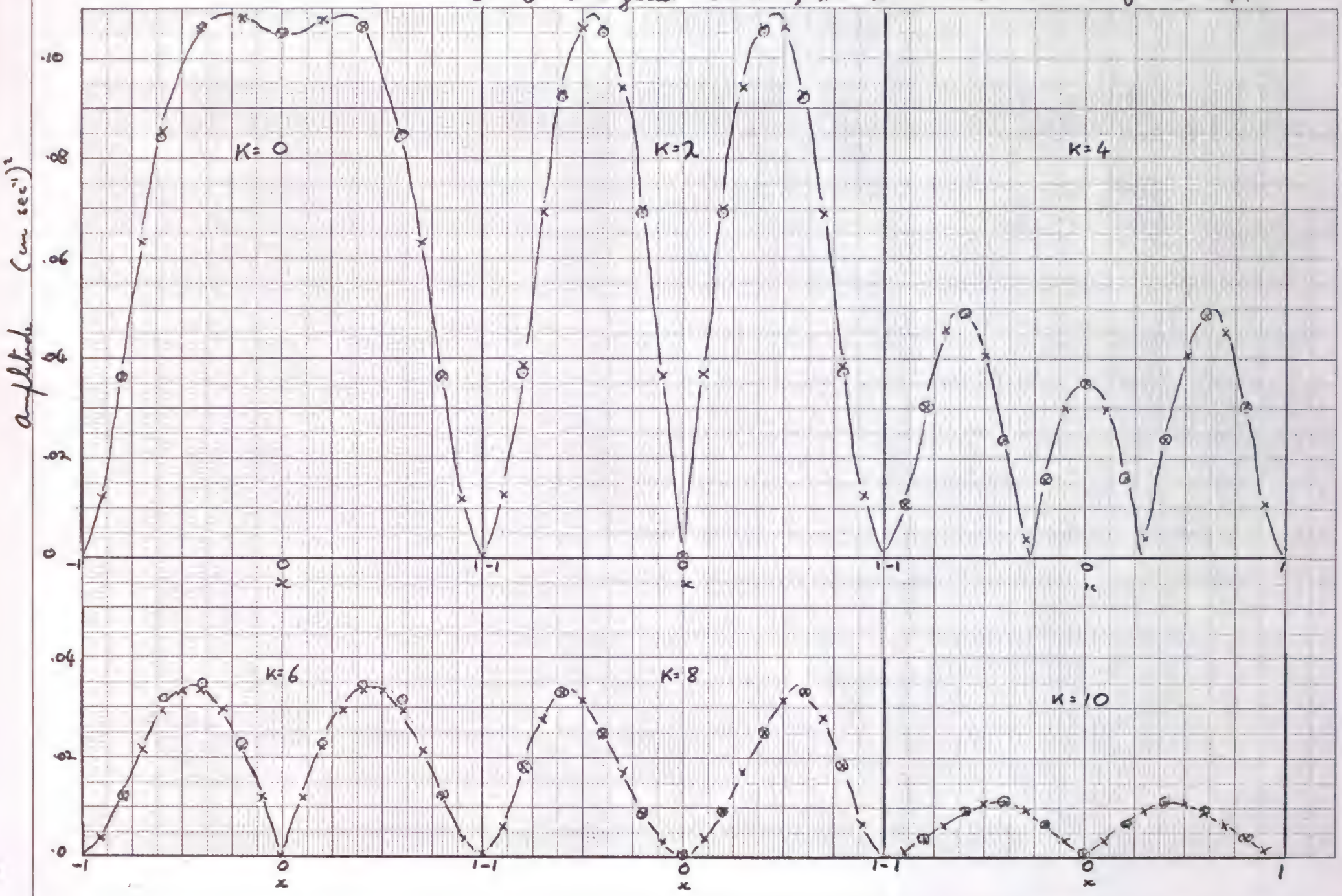

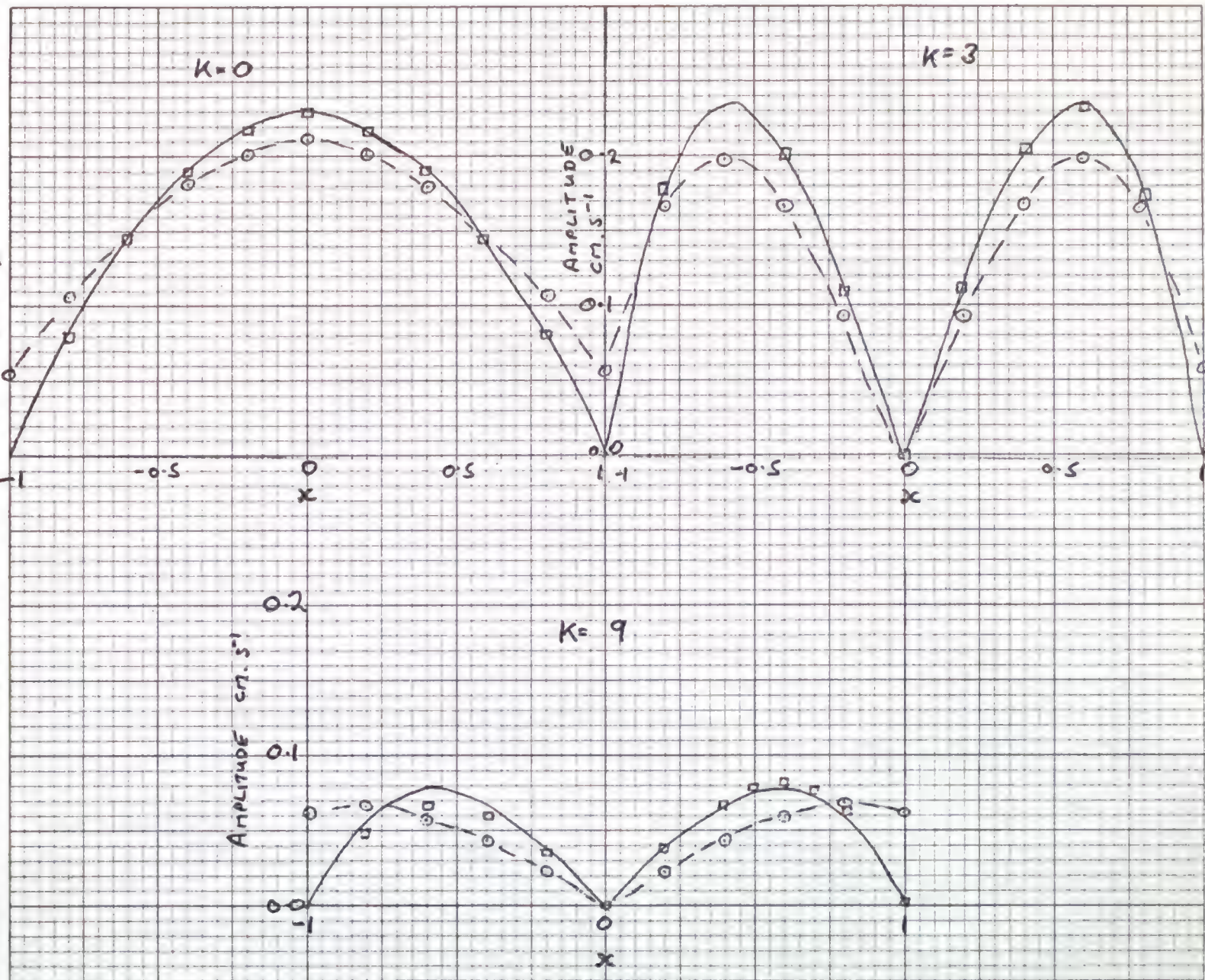

Figure 3.1

Simulated flow of wave number 3. analysis of zonal component of velocity. Comparison of different data, —— analytical solution, o—o 3rd order polynomial amplitudes, □ □ solution with 5th order polynomial with amplitude zero at $x = \pm 1.0$.

RECONSTRUCTION OF STREAK PHOTOS BEFORE AND AFTER ANALYSIS

RUN 4A SIM 2A ITER=4 NDA=250 USE=167

INITIAL SET OF VELOCITIES

DERIVED SET OF VELOCITIES

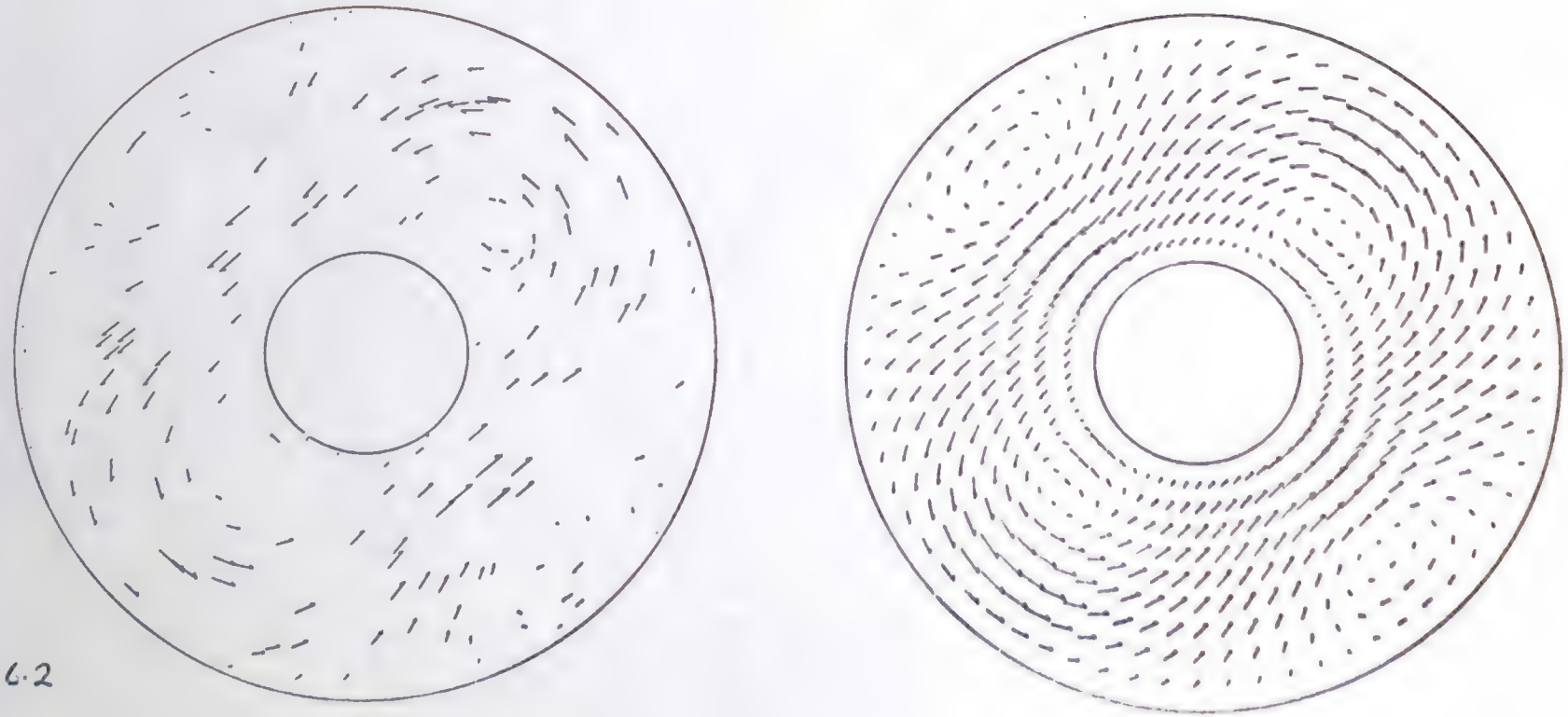

Figure 6.2

RECONSTRUCTION OF STREAK PHOTOS BEFORE AND AFTER ANALYSIS

RUN 7 SIM 5A ITER=4 NDA=239 USE=173

INITIAL SET OF VELOCITIES

DERIVED SET OF VELOCITIES

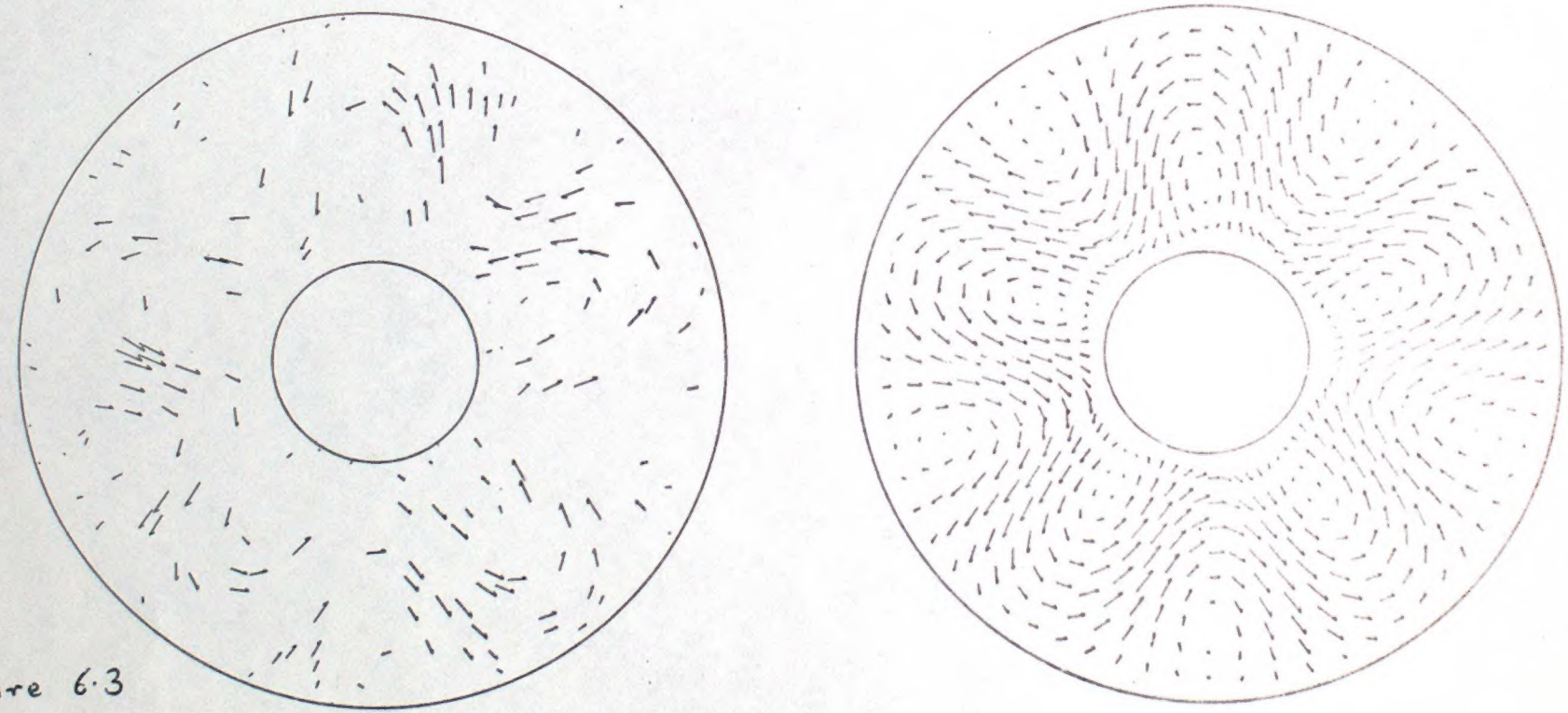

Figure 6.3

RECONSTRUCTION OF STREAK PHOTOS BEFORE AND AFTER ANALYSIS

RUN 3 SIM 2.4 ITER=10 NDA=239 USE=170

INITIAL SET OF VELOCITIES

DERIVED SET OF VELOCITIES

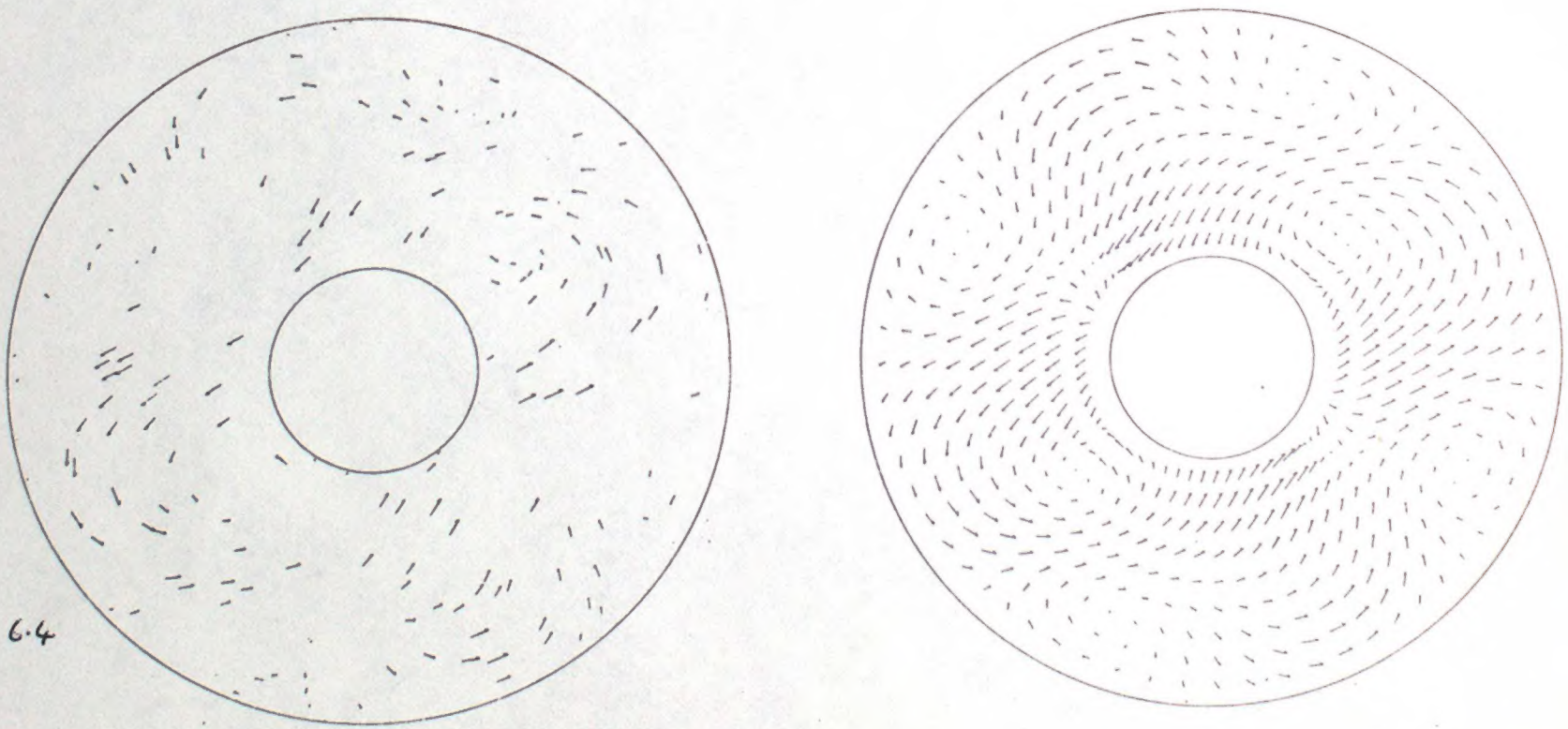

Figure 6.4

Figure 6.5

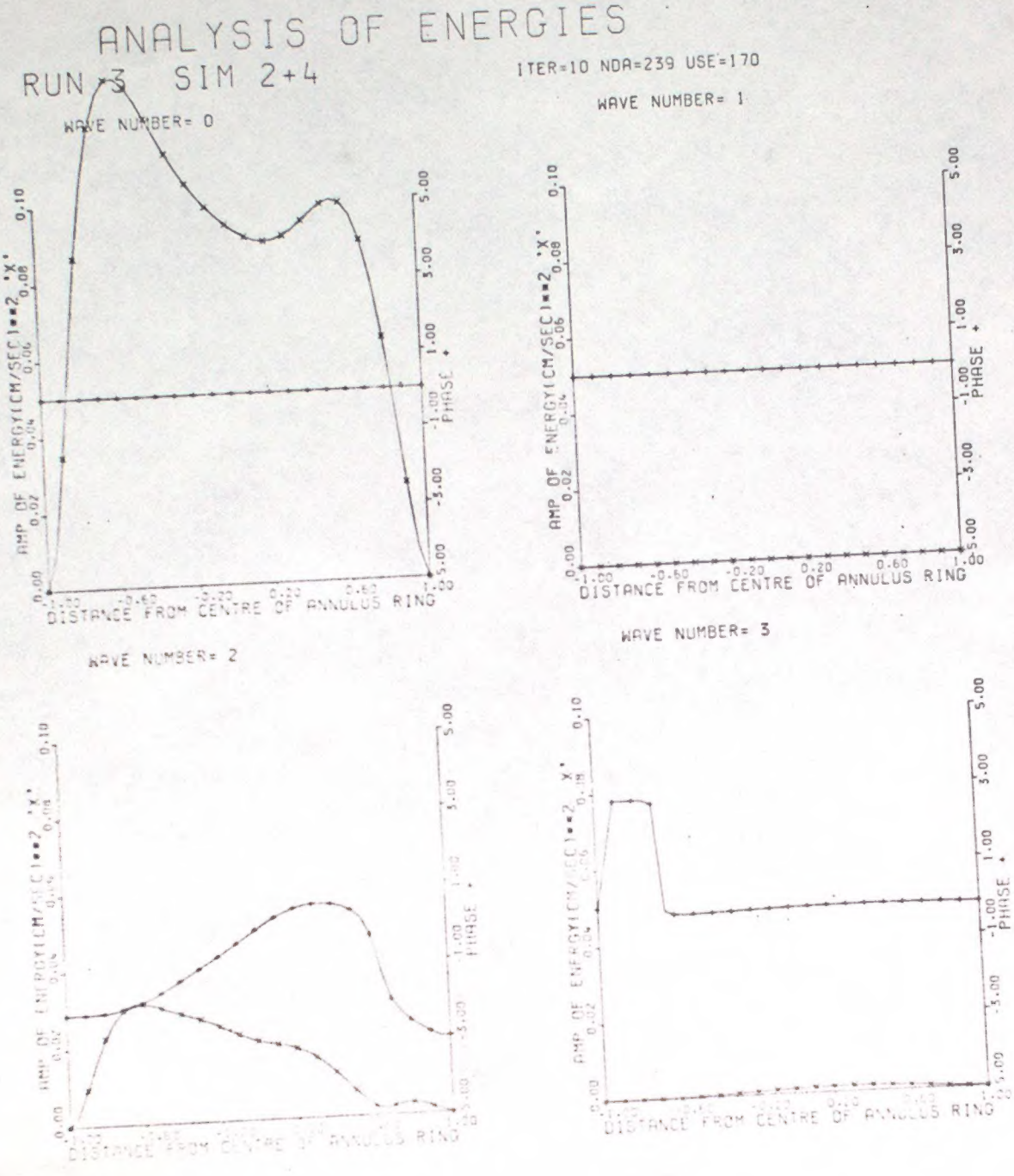
ANALYSIS OF ENERGIES
RUN =3 SIM 2+4
ITER=10 NDA=239 USE=170
WAVE NUMBER= 0
WAVE NUMBER= 1
WAVE NUMBER= 2
WAVE NUMBER= 3
AMP OF ENERGY(CM/SEC)**2 'X'
PHASE
DISTANCE FROM CENTRE OF ANNULUS RING

Figure 6.6

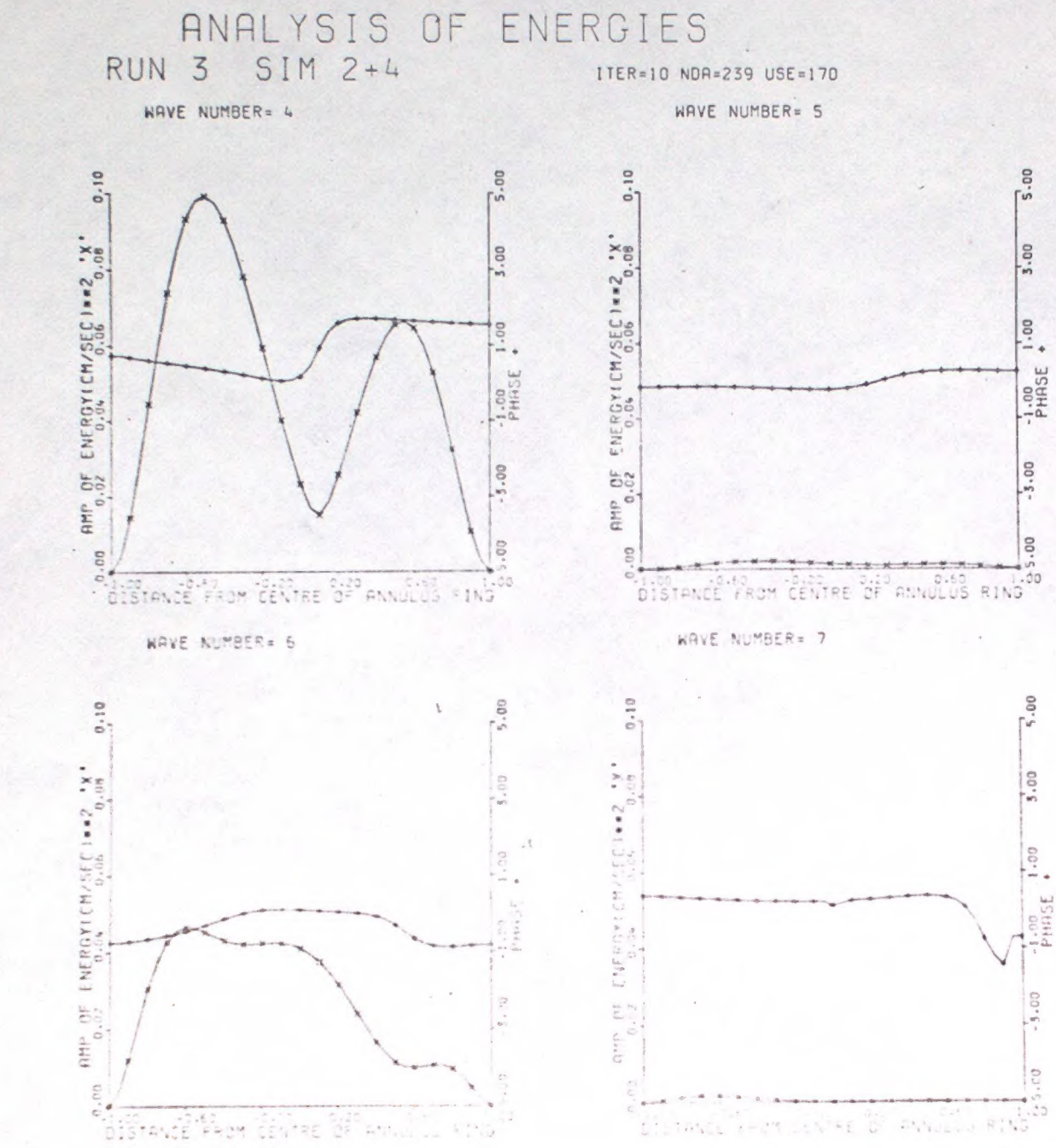
ANALYSIS OF ENERGIES
RUN 3 SIM 2+4
ITER=10 NDA=239 USE=170
WAVE NUMBER= 4
WAVE NUMBER= 5
WAVE NUMBER= 6
WAVE NUMBER= 7
AMP OF ENERGY(CM/SEC)**2 'X'
PHASE
DISTANCE FROM CENTRE OF ANNULUS RING